Italian Journal of Engineering Geology and Environment
www.ijege.uniroma1.it

TREND ANALYSIS OF SNOW COVER CHANGES USING STATISTICAL DOWNSCALING MODEL AND CLIMATE SCENARIOS IN SEFID-RUD BASIN (IRAN)

Hersh ENTEZAMI(*), Firouz MOJARRAD(*),
Mohammad DARAND(**) & Ebrahim GHADERPOUR(***)

(*)Razi University - Faculty of Literature and Humanities - Department of Geography - Tagh Bostan, Kermanshah, Iran
(**)University of Kurdistan - Department of Climatology, Faculty of Natural Resources - Sanandaj, Iran
(***)Sapienza University of Rome - Department of Earth Sciences & CERI Research Centre - Rome, Italy
Corresponding author: f_mojarrad@razi.ac.ir; ebrahim.ghaderpour@uniroma1.it

EXTENDED ABSTRACT

La copertura nevosa può potenzialmente bilanciare la temperatura della superficie terrestre e riempire fiumi e bacini idrici durante la stagione primaverile. I cambiamenti climatici influiscono sulla profondità, sulla massa e sull'estensione della neve, con il risultato che le aree montuose sono più vulnerabili alla pioggia e ai cambiamenti di temperatura. La neve è un'importante fonte di umidità del suolo durante la stagione primaverile. La fusione della neve consente il ripristino graduale delle riserve idriche sotterranee e fornisce approvvigionamento idrico per l'agricoltura, l'industria e l'uso civile. Pertanto, il monitoraggio e la previsione del manto nevoso e dei suoi fattori influenti, come il vento e la temperatura, sono molto importanti per la gestione ambientale e il mantenimento di un ambiente sostenibile.

L'Iran ha precipitazioni relativamente più basse rispetto ad altre regioni del mondo e ha una condizione climatica arida/semi-arida. Avendo una popolazione elevata e una domanda idrica molto elevata, è fondamentale controllare e gestire le risorse idriche del Paese. Il bacino idrografico di Sefid-Rud è uno dei più grandi bacini dell'Iran. Questo bacino ha una superficie di circa 59.000 km^2, situato nella parte nord-occidentale dell'Iran. Il fiume principale di questo bacino è il Sefid-Rud, il secondo più lungo dell'Iran, la cui lunghezza è di circa 750 km. In una precedente pubblicazione, gli autori hanno stimato la tendenza della copertura nevosa del bacino di Sefid-Rud e dei suoi sottobacini su scala mensile, stagionale e annual, utilizzando l'analisi non parametrica di Mann-Kendall e la pendenza di Sen associata. E' stato rilevato che il calo più significativo del manto nevoso si è verificato nella stagione invernale, ovvero dicembre, gennaio e febbraio. Inoltre, si è osservato un aumento delle praterie e una diminuzione delle aree non vegetate, principalmente verso la parte centrale del bacino.

Nel presente studio, viene indagato l'impatto dei parametri climatici sui cambiamenti della copertura nevosa nel bacino di Sefid-Rud e nei suoi 11 sottobacini, utilizzando il modello del Sistema Terra canadese di seconda generazione (CanESM2) che ha 26 diversi predittori di parametri climatici per i periodi storici e futuri. Per illustrare i risultati in modo più dettagliato, è stato selezioniamo un pixel in ogni sottobacino. Viene determinato il parametro climatico più efficace nelle variazioni della copertura nevosa per il periodo 2000-2005 e quindi convalidato l'effetto dei risultati sui modelli di variazione della copertura nevosa. Sono poi confrontati i risultati del periodo 2006-2019 con il manto nevoso ottenuto dalle immagini satellitari. Inoltre, sono riportati in forma tabellare i parametri climatici statisticamente significativi per gli 11 pixel selezionati.

Dopo aver determinato i parametri più significativi che influenzano la copertura nevosa del bacino di Sefid-Rud, sono effettuate previsioni sulla copertura nevosa in tutto il bacino fino al 2100 in tre diversi scenari ipotizzati di eventuale cambiamento climatico, ovvero RCP 2.6, RCP 4.5 e RCP 8.5. Per prevedere la copertura nevosa nel bacino di Sefid-Rud parametri climatici viene utilizzato un modello statistico di downscaling. Inoltre, è utilizzato il modello dei minimi quadrati per stimare una tendenza lineare che si adatta meglio a ciascuna serie temporale della copertura nevosa durante il 2020-2100 per dicembre, gennaio e febbraio nei tre scenari di cambiamento climatico. E' riportata anche la significatività statistica (*p-value*) dei tassi di copertura nevosa stimati per il periodo 2020-2100 per gli 11 pixel selezionati in tre tabelle, corrispondenti a dicembre, gennaio e febbraio. Inoltre, sono illustrate le serie temporali del manto nevoso corrispondenti a uno dei pixel selezionati per una migliore comprensione e visualizzazione. Controllando i parametri climatici che influenzano in modo significativo l'area nevosa nei diversi sottobacini, emerge che il numero di questi parametri varia da 2 a 6 su 26. Tuttavia, parametri come la temperatura, la velocità del vento in superficie e nei livelli più alti dell'atmosfera, la direzione della velocità del vento in superficie e a quote più elevate e l'umidità assoluta sono i parametri più frequenti e influenti. La temperatura risulta essere il parametro climatico più influente sui cambiamenti della copertura nevosa in 9 degli 11 pixel selezionati. Nello scenario RCP2.6 si osserva un aumento del manto nevoso. Tuttavia, nei due scenari ipotizzati, RCP4.5 e RCP8.5, le previsioni del manto nevoso mostrano una tendenza alla riduzione a causa della tendenza al riscaldamento specie nel caso RCP8.5. Nel complesso, si prevede che la copertura nevosa in tutto il bacino diminuirà in futuro a causa del riscaldamento globale e dei risultati ottenuti dalle diverse fasi di questa ricerca. Confrontando i risultati con altri studi, si conferma anche il ruolo del cambiamento climatico nella riduzione della copertura nevosa in tutto il bacino.

IJEGE, 2 (2024): 77-86, DOI: 10.4408/IJEGE.2024-02.O-07
E-ISSN 2035-5688 | ISSN 1825-6635 / ©Author(s)

ABSTRACT

Investigating the status of snow cover and possible changes due to climate change is a vital and important issue. In the present study, snow cover change trends, possible effect of climatic parameters on these changes and future forecasts of snow cover of Sefid-Rud Basin are investigated using 8-day MOD10A2 products of moderate resolution imaging spectroradiometer (MODIS) sensor for the period 2000-2019. After preparing the snow cover map of all the images of the study period, the percentage of snow cover is determined. In each of the 11 subbasins, one pixel is selected to demonstrate the results in more detail. Then based on the climate parameters of the CanESM2 climate model from the fifth climate change report (FCCR) and utilizing the statistical downscaling model (SDSM), climate parameters effective in changes of snow cover of the 11 pixels for the period of 2000-2005 are determined. To validate the effect of these results on snow cover change patterns, the results of the 2006-2019 period are compared with the snow cover obtained from satellite images. Finally, by determining the relationship between climatic parameters and snow cover and according to the scenarios of FCCR, the snow cover of the 11 pixels is calculated for the period 2020-2100. The study of the effect of CanESM2 climatic parameters on snow cover shows that at all 11 pixels, several climatic parameters, particularly temperature and wind speed, impacted the snow cover change patterns. Therefore, to predict future snow cover, climatic data are used based on the scenarios, indicating that snow cover would decrease sharply based on the two scenarios RCP4.5 and RCP8.5, particularly RCP8.5. The results of the model validation and comparison with satellite data show that the accuracy of the SDSM in predicting snow cover is acceptable.

Keywords: *snow cover, MODIS, CanESM2, downscaling, Sefid-Rud Basin, Iran*

INTRODUCTION

The amount of snowfall and the seasonal spatial and temporal variability of the amount of snow cover (SCE) greatly impact the hydrological balance in the cryosphere (Malmros *et alii*, 2018). The timing and spatial distribution of snow cover through its accumulation phase and melting cycle have affected many vital and non-vital processes of the earth and they are crucial decision-makers in hydrological systems, energy balance, environmental characteristics and global climate changes. (Salomonson & Apple, 2004; Cohen *et alii*, 2015; Moore, 2011). The reduction or expansion of snow cover during a period in a place proves the existence of changes in that place and is considered an indicator of climate change (Singh *et alii*, 2018). Investigating the amount of snow cover and its continuity are a reliable indicator to prove climate change trends (Shuai *et alii* 2011; IPCC, 2013).

Several studies have reported the downward and sometimes upward trend of snow covers around the world in response to climate change (Muntan *et alii*, 2009; Zhao *et alii*, 2009; Sharma *et alii*, 2012; Pachauri *et alii*, 2014; Entezami *et alii*, 2024). Much attention has been focused on investigating the effects of climate change on snow cover and hydrological regime worldwide. Climate changes impact the depth, mass and extent of snow, which ultimately result in mountains being more vulnerable to rain and temperature changes (Vanham, 2012; Laghari *et alii*, 2012).

According to the report of the Intergovernmental Panel on Climate Change, the average temperature of the earth's surface and sea surface shows an increase of approximately 0.89 degrees Celsius between 1901 and 2012 (Rani, 2017). Due to the premature melting of snow cover and the movement of melting snow runoff from spring to winter, there is a possibility of increasing winter floods and summer drought (Ahmad *et alii*, 2018).

It has been proven that remote sensing is an effective technique for studying snow characteristics at the local and global levels, particularly due to the vastness of snow areas and difficulties in obtaining ground estimates in cold regions (Kulkarni *et alii*, 2011; Pant *et alii*, 2014; Tahir *et alii*, 2015). Satellite remote sensing methods for preparing the snow cover map, developed in the 1960s, have improved over time with the availability of data with favorable spatial and temporal resolutions (Dietz *et alii*, 2012). The moderate resolution imaging spectroradiometer (MODIS) is a reliable sensor on board Terra and Aqua satellites frequently used for environmental and climate change monitoring (Aghelpour *et alii* 2020; Ghaderpour *et alii* 2023, 2024). These satellites provide images of the entire Earth every 1 to 2 days with high radiometric sensitivity though they have moderate resolution (250 m, 500 m, 1 km). MODIS, like other optical satellite sensors, cannot observe the Earth's surface when cloud cover is present. Therefore, there are often gaps and uncertainties in MODIS images due to clouds which can significantly impact the analysis, and so statistical pre-processing and gap-filling models are required to enhance the image quality and reliability (Ahmed *et alii*, 2023; Arabi Aliabad *et alii*, 2024).

Compared to the world average, Iran has very little rainfall and climatically, dry and semi-arid conditions prevail over most of its regions. Under these conditions and with the increase in population and greater demand for water in the country, it is vital to control and manage the country's water resources. In this regard, the investigation of the country's snow reserves, and its change process is of high importance since these reserves are a vital source of water used for various purposes.

Entezami *et alii* (2024) estimated and illustrated the snow

cover trend maps for the Sefid-Rud basin and its sub-basins for the period 2000-2019 at monthly, seasonal, and annual scales using MODIS snow cover products. They showed that the most significant reduction of snow cover has occurred in the winter season, *i.e.*, December, January, and February. They also observed an increase in grasslands and decrease in non-vegetated lands, mainly toward the central part of the basin. However, their study did not discuss the relationships between climate change and snow cover historically nor for the future. In the present research, snow changes trends in the Sefid-Rud watershed which is one of the most important watersheds of Iran are investigated. Examining the possible impact of climate change on the amount of snow reserves and future pattern of change will enable excellent decision making in the optimal management of these resources. The main contributions of the present research are:

- Investigating the influence of climatic parameters on snow cover changes.
- Forecasting the snow cover of the Sefid-Rud basin to 2100 under three different climate change scenarios, *i.e.*, RCP 2.6, RCP 4.5, and RCP 8.5.
- Estimating the trends of the snow cover time series during 2020-2100 for December, January, and February under the three climate change scenarios.

The remainder of this paper is organized as follows: Section 2 describes the study region and datasets. Section 3 describes the methods. Section 4 presents the results, and Section 5 briefly discusses the results and concludes this research.

MATERIALS

Study region

The study region is the Sefid-Rud basin, one of the largest watersheds in Iran and a subset of the Caspian Sea regional basin. This basin, with an area of more than 59,000 km^2, is within the longitudes of 46 degrees and 31 minutes to 51 degrees and 4 minutes east and latitudes of 34 degrees and 54 minutes to 37 degrees and 49 minutes north (Figure 1). Its main river is Sefid-Rud, the second longest river in Iran, with a length of 750 km and the largest river in the north of Iran, formed by the combination of the two rivers of Shahrud and Qezel-Ozan.

The Sefid-Rud basin consists of 11 subbasins, the Mianeh is the largest and the Manjil is the smallest sub-basin. There is a great height variation in this basin. Based on this, the Astaneh-Kochsefahan subbasin with a height of -28 meters on the coast of the Caspian Sea has the lowest elevation and the Taleghan-Alamot subbasin in the Alborz Mountain with about 4357 meters has the highest elevation. Meanwhile, the highest frequency of altitude in the basin is in the altitude classes of 1600-2000 meters.

Due to the Zagros and Alborz Mountains and plains and flat areas, such as the beaches of the Caspian Sea in this basin, the changes in the slope have been severe which can be seen from 0 degrees to 69 degrees. The most common slope of the basin is between 0-3 degrees. In terms of slope direction, north and south directions are the most frequent. The annual average precipitation and temperature in the basin are approximately 1500 mm and 16°C, respectively (Entezami *et alii*, 2024). The summers are usually warm and dry, reaching temperature of 30°C while the winters are usually cold and wet.

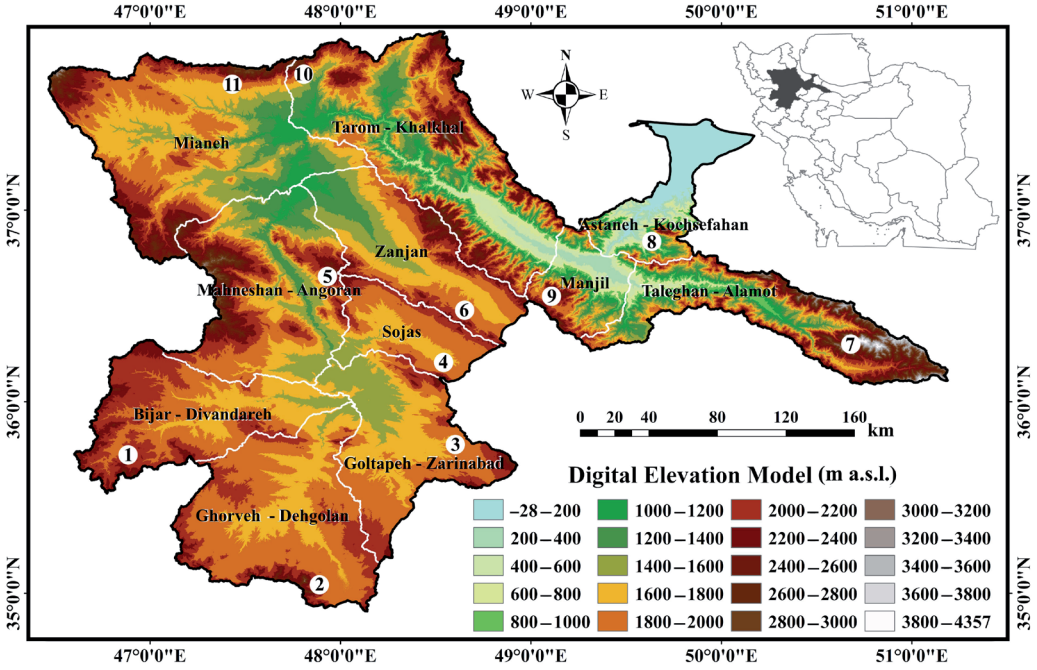

Fig. 1 - Map of the Sefid-Rud basin and its sub-basins and the locations of 11 samples pixels

Datasets

- MODIS images

MODIS products of snow cover are employed to determine the extent of snow. For this purpose, 8-day MOD10A2 snow cover images of resolution 500 m are downloaded from the NASA website (DOI: 10.5067/MODIS/MOD10A2.006) for the period 2000-2019. The quality assessment band is used to mask the low quality pixels due to clouds and atmospheric noise (Riggs *et alii*, 2019).

- Climate model data

Climate models are utilized to find the correlation between past and future changes in the snow area of the basin. The second generation Canadian Earth System model (CanESM2) is used (Boudala *et alii*, 2022), which has 26 different predictors of atmospheric parameters for the historical and future periods. Table 1 summarizes the list of parameters in CanESM2, used in the present study for sensitivity analysis.

Number	Name Parameter's	Parameter Definition	SI Unit
1	ces2mslpgl	Mean sea level pressure	Pa
2	ces2p1 fgl	Wind speed at the level of 1000 hPa	m/s
3	ces2p1 ugl	Orbital wind component at the level of 1000 hPa	m/s
4	ces2p1 vgl	The component of the meridian wind at the level of 1000 hPa	m/s
5	ces2p1 zgl	Relative rotation of the real wind at the level of 1000 hPa	1/s
6	ces2p1thgl	Wind direction at the level of 1000 hPa	degree
7	ces2p1zhgl	Actual wind divergence at 1000 hPa level	1/s
8	ces2p5 fgl	Wind speed at the level of 500 hPa	m/s
9	ces2p5 ugl	Orbital wind component at the level of 500 hPa	m/s
10	ces2p5 vgl	The component of the meridian wind at the level of 500 hPa	m/s
11	ces2p5 zgl	Relative rotation of the real wind at the level of 500 hPa	1/s
12	ces2p5thgl	Wind direction at the level of 500 hPa	degree
13	ces2p5zhgl	Actual wind divergence at 500 hPa level	1/s
14	ces2p8 fgl	Wind speed at the level of 850 hPa	m/s
15	ces2p8 ugl	Orbital wind component at the level of 850 hPa	m/s
16	ces2p8 vgl	The component of the semi-diurnal wind at the level of 850 hPa	m/s
17	ces2p8 zgl	Relative rotation of the real wind at the level of 500 hPa	1/s
18	ces2p8thgl	Wind direction at the level of 850 hPa	degree
19	ces2p8zhgl	Actual wind divergence at 850 hPa	1/s
20	ces2p500gl	Surface geopotential of 500 hPa	m
21	ces2p850gl	Surface geopotential at 850 hPa	m
22	ces2prcpgl	Total precipitation	mm
23	ces2s500gl	Specific humidity at the level of 500 hPa	kg/kg
24	ces2s850gl	Specific humidity at the level of 850 hPa	kg/kg
25	ces2shumgl	Specific humidity at the level of 1000 hPa	kg/kg
26	ces2tempgl	Air temperature at a height of 2 m	°C

Tab. 1 - List of parameters in CanESM2

METHODS

Investigating the Influence of Climatic Parameters on Snow Cover Changes

For this research, 11 pixels, each in a different subbasin, are selected as an example. The locations of these pixels are highlighted in Figure 1. The amount of snow cover during 2000-2019 is calculated for 11 pixels using the downloaded satellite images. To investigate the relationship between snow area changes and climate parameters, CanESM2 data from the fifth climate change report (CMIP5) are employed.

Considering that the historical data of CanESM2 are for the period up to the year 2005 and the future data are from 2006 onwards, the images of 2000 to 2005 are used to investigate and determine the relationship between the snow area and climate parameters and the images of 2006 to 2019 are used for the validation. Then the correlation between the snow area of these points and the climate parameters of CanESM2 is examined using statistical downscaling model (SDSM) and linear regression in SPSS (statistical package for the social sciences) software.

- Coupled Model Intercomparison Project 5 (CMIP5)

A group of dynamic models of the general circulation of the atmosphere approved by the World Climate Research Programme (WCRP) working group of the World Meteorological Organization is known as the CMIP5 model. The title CMIP is a name given by the Intergovernmental Panel on Climate Change (IPCC) to a number of atmospheric general circulation models. For example, CMIP5 refers to a group of approximately 40 general circulation models with appropriate accuracy that are used in the preparation of the fifth report of the IPCC. By conducting tests based on models with higher spatial resolution, these models improve the features of the model, and its output information is richer and more qualitative than the previous phases (Taylor *et alii*, 2012). In addition, the presentation of the image of climate change by CMIP5 is based on new climate scenarios that use the time series of emissions and concentrations of greenhouse gases (RCPs). Therefore, atmospheric general circulation models by CMIP5 have been widely used in climate change assessments (Gulizia & Camilloni, 2015).

- Statistical Downscaling Model (SDSM)

In SDSM, statistical relationships between large-scale variables (predictors) and local variables (predictors) are established based on the multiple linear regression method, used for long-term forecasting of climate parameters, such as precipitation and temperature. These relations are established by using the observational data of the ground station and the values presented (output) of the general circulation models in the same period of observation. Before performing the downscaling process in this model, observational data and general circulation model data are normalized based on their average values and standard deviation for the desired period. The reason for data normalization is that atmospheric general circulation models cannot simulate the local climate as well as observational data. Therefore, an unrealistic correlation will be created, if they are compared before normalization. Predictive variables provide large-scale atmospheric information while the predicted variables determine the state of the atmosphere at a point/local scale. Since the method used in this model is a combination of probabilistic and regression methods, it has a high importance and position among different models (Khan *et alii*, 2006).

Prediction of snow cover using climate scenarios

After determining the parameters that affect the snow area of each pixel and determining their regression relationships, using the climate parameters of the three scenarios of RCP2.6, RCP4.5, and RCP8.5 of CanESM2 model data between 2006 and 2100, the snow area at these points is predicted for upcoming years. Because

the snow area of the studied basin for the years 2006 to 2019 is calculated through available satellite images, the calculated snow area is compared with the snow area predicted by the model to determine the prediction accuracy and validation of the used model.

Finally, the forecasted snow area using climate parameters in three CMIP5 scenarios for 2020-2100 is checked and possible decreases or increases in snow area trends are determined using linear regression relationships (Ahmed *et alii*, 2023). The slope (m) and intercept (b) of a linear line are estimated by minimizing the residual series using the least-squares method. Furthermore, to test whether the estimated slope ($\hat{m}$) is statistically significant, the test statistics $t = \hat{m}/E$ is formed, following the student's t-distribution, where E is the standard error of the estimated slope (Zaghloul *et alii*, 2022).

The Fifth Report of the Inter-State Panel was presented in 2010, where RCP scenarios replaced Special Report on Emissions Scenarios (SRES) scenarios. Climate models use the results of these scenarios to show the concentration and emission of greenhouse gases and land use changes. This series introduced scenarios, RCP2.6, RCP4.5, and RCP8.5, based on different characteristics, such as the level of technology and future socio-economic conditions which lead to different levels of greenhouse gas emissions and climate changes in each situation.

RESULTS

Results of the effect of climatic parameters on snow cover changes

The 11 pixels numbered in Figure 1 are considered for investigating snow reserve changes and comparing SDSM with the historical climate parameters of CanESM2 of FCCR of 2000-2005. According to the results, there is a significant regression correlation between the snow area and some climatic parameters in most of the pixels, and there is a significant correlation with one or two parameters in some of the selected pixels. The type of parameter varies in different stations. However, the parameter of temperature (ces2tempgl) is influential in almost all stations. To exemplify, the results of the regression relationships between the snow area and the climatic parameters of 11 pixels are shown in Table 2.

Since this model and its regression relationships are implemented at the 95% confidence level, for the effect of any parameter on snow cover to be significant, this value must be smaller than 0.05 (5%). The smaller this value is, the higher the confidence percentage will be. In the obtained results, these values are all close to zero, indicating the significance of the relationship between them. In Table 2, Column B shows the constant number of regression relationships for each variable, and column Beta is the coefficient of the desired variable in the relationship.

To validate the results of using CanESM2 and the regression relationships obtained for the tested pixels, the snow area is forecast for the years 2006-2019 according to the three scenarios RCP2.6, RCP4.5 and RCP8.5. These pixels are compared with real snow surface data. Examining the results using the root mean square error (RMSE) obtained between 0.2 and 0.4 shows that the predictions are largely acceptable and confirmed. The results show

Pixel 1	Unstandardized Coefficients		Standardized	t-value	p-value
	Average (B)	Std. Error	Coefficients (Beta)		
Constant	-205.458	48.442	-----	-4.241	0
ces2p1_fgl	222.332	20.895	0.939	10.64	0
ces2p5_ugl	-67.284	8.901	-1.033	-7.559	0
ces2p5thgl	1.053	0.2	0.802	5.267	0
ces2shumgl	-52.315	5.792	-0.727	-9.032	0
Pixel 2	**Unstandardized Coefficients**		**Standardized**	**t-value**	**p-value**
	Average (B)	**Std. Error**	**Coefficients (Beta)**		
Constant	159.04	27.18	-----	5.85	0
ces2p1_fgl	105.33	23.34	0.78	4.51	0
ces2p1_vgl	-43.19	11.29	-0.42	-3.83	0
ces2p5thgl	-0.52	0.11	0.43	-4.63	0
ces2shumgl	-11.33	4.83	0.17	-2.35	0.023
ces2tempgl	-43.91	5.03	-1.04	-8.73	0
Pixel 3	**Unstandardized Coefficients**		**Standardized**	**t-value**	**p-value**
	Average (B)	**Std. Error**	**Coefficients (Beta)**		
Constant	33.94	4	----------	4.48	0
ces2p1_fgl	116.4	30.12	0.52	3.86	0
ces2p1_vgl	-50.21	14.88	-0.47	-3.37	0.001
ces2shumgl	-25.17	5.72	-0.37	-4.4	0
ces2tempgl	-31.44	6.31	-0.73	-4.98	0
Pixel 4	**Unstandardized Coefficients**		**Standardized**	**t-value**	**p-value**
	Average (B)	**Std. Error**	**Coefficients (Beta)**		
Constant	45.125	4.389	--------	10.282	0
ces2p1_fgl	172.819	22.698	0.729	7.614	0
ces2shumgl	-34.098	6.899	-0.474	-4.943	0
Pixel 5	**Unstandardized Coefficients**		**Standardized**	**t-value**	**p-value**
	Average (B)	**Std. Error**	**Coefficients (Beta)**		
Constant	29.37	28.226	----------	1.041	0.303
ces2tempgl	-43.587	3.201	-1.054	-13.619	0
ces2p1_fgl	82.383	10.848	0.434	7.594	0
ces2p8_vgl	-113.007	10.92	-1.131	-10.348	0
ces2p5thgl	-0.538	0.164	-0.269	-3.273	0.002
ces2p8thgl	0.843	0.145	0.733	5.799	0
ces2prcpgl	1.315	0.288	0.256	4.559	0
Pixel 6	**Unstandardized Coefficients**		**Standardized**	**t-value**	**p-value**
	Average (B)	**Std. Error**	**Coefficients (Beta)**		
Constant	27.864	2.367	----------	11.771	0
ces2tempgl	-54.528	3.545	-1.391	-15.38	0
ces2p1_fgl	38.222	11.898	0.212	3.212	0.002
ces2p8_vgl	-55.25	8.907	-0.583	-6.203	0
ces2p850gl	-19.335	5.239	-0.308	-3.69	0.001
Pixel 7	**Unstandardized Coefficients**		**Standardized**	**t-value**	**p-value**
	Average (B)	**Std. Error**	**Coefficients (Beta)**		
Constant	54.104	1.884	----------	28.712	0
ces2p1_vgl	66.048	7.483	0.616	8.826	0
ces2p5_ugl	-25.563	3.043	-0.393	-8.4	0
ces2tempgl	-22.601	3.124	-0.494	-7.234	0
Pixel 8	**Unstandardized Coefficients**		**Standardized**	**t-value**	**p-value**
	Average (B)	**Std. Error**	**Coefficients (Beta)**		
Constant	13.038	3.148	----------	4.141	0
ces2p8_vgl	-33.695	10.251	-0.299	-3.287	0.002
ces2tempgl	-23.3	2.743	-0.772	-8.494	0
Pixel 9	**Unstandardized Coefficients**		**Standardized**	**t-value**	**p-value**
	Average (B)	**Std. Error**	**Coefficients (Beta)**		
Constant	31.264	2.982	---------	10.485	0
ces2tempgl	-35.675	3.023	-0.838	-11.803	0
Pixel 10	**Unstandardized Coefficients**		**Standardized**	**t-value**	**p-value**
	Average (B)	**Std. Error**	**Coefficients (Beta)**		
Constant	-58.52	21.973	----------	-2.663	0.01
ces2tempgl	-33.379	3.438	-0.739	-9.708	0
ces2p5_fgl	-44.36	6.631	-0.534	-6.69	0
ces2p8thgl	0.594	0.131	0.473	4.545	0
Pixel 11	**Unstandardized Coefficients**		**Standardized**	**t-value**	**p-value**
	Average (B)	**Std. Error**	**Coefficients (Beta)**		
Constant	202.98	30.27	----------	6.7	0
ces2p1_fgl	38.9	10.71	0.2	3.63	0.001
ces2p5thgl	-0.92	0.18	-0.45	-4.97	0
ces2p8thgl	0.35	0.15	0.3	2.4	0.02
ces2tempgl	-32.91	3.47	0.77	-9.49	0

Tab. 2 - Regression relationships between snow cover and climatic parameters (see Table 1) in the 11 pixels whose geographic locations are highlighted in Fig. 1

that the estimated snow cover is more like the RCP8.5 scenario which is a pessimistic scenario and its RMSE error is better than RCP2.6 and RCP4.5 scenarios. The existence of the error can be related to the fact that the snow cover area is zero on many days of the year leading to a reduction in the accuracy of the results.

Snow cover forecast results using climate scenarios

The snow area for the years 2020-2100 is predicated and its changes investigated using CanESM2 climate data related to FCCR and the three scenarios of RCP2.6, RCP4.5 and RCP8.5. Therefore, using these cases, the snow area of 11 study pixels is calculated as a representative of different areas of the study basin until the year 2100 in the above-mentioned three scenarios. For brevity, only the results of one pixel (#5 in Figure 1) are illustrated in Figure 2.

By examining the graphs of the three scenarios for the next 80 years, the accuracy of the model can be confirmed. The similarity of the graphs of the three scenarios in terms of the rises and falls due to seasonal changes and its harmony with the seasons are reasons for their confirmation. While there is a difference between the values of the different scenarios, the increases and decreases in the charts because of seasonal changes are similar and logical. The percentage of snow cover in the warmer half of the year usually

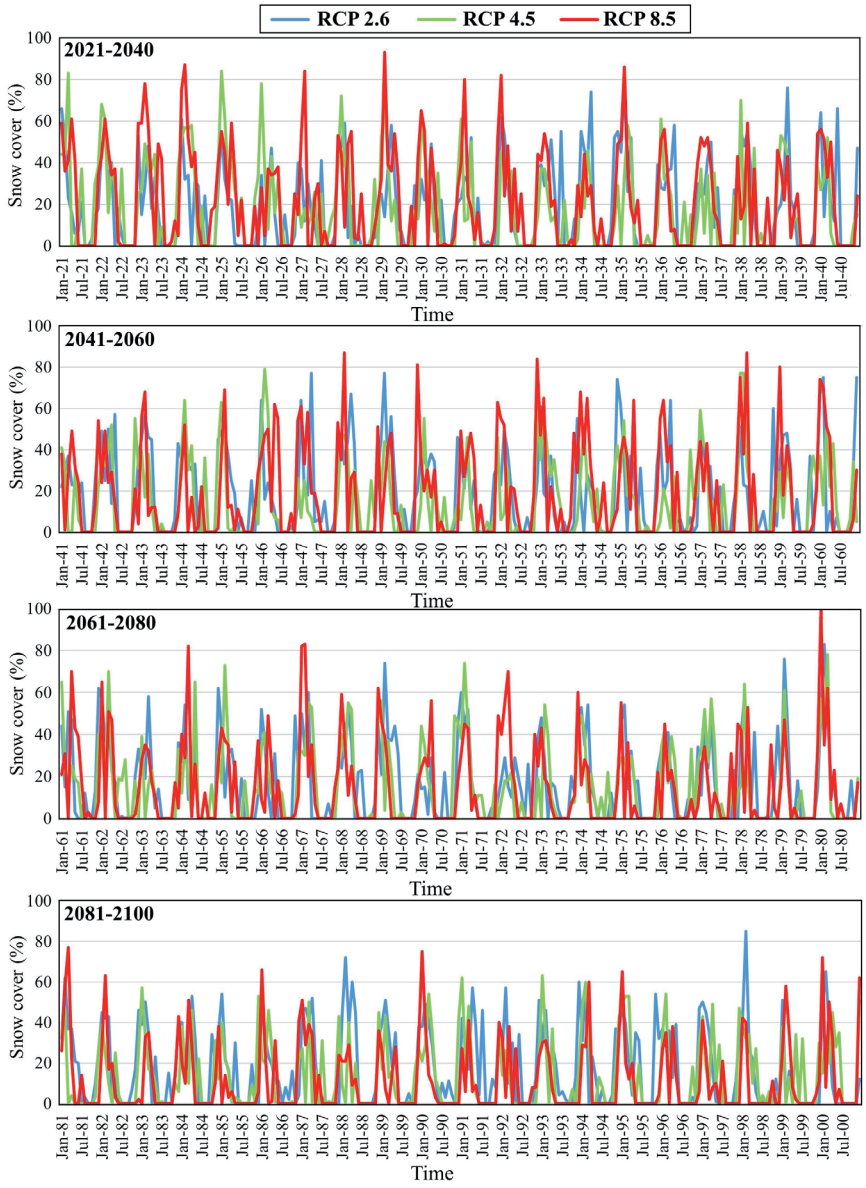

Fig. 2 - Monthly snow cover forecast for the 2020-2100 according to the three climate change scenarios for pixel #5 located in Mahneshan-Angoran sub-basin, shown in Figure 1

reaches zero or close to zero, which can be seen in the forecast made by the model for the upcoming years. The graphs in the three scenarios for the summer season show the zero value of all years.

According to Figure 2, future snow cover change pattern fluctuated, which is a normal occurrence. However, an examination of the RCP8.5 diagram reveals that the percentage of snow cover decreases with time, particularly in the last years of the period.

Snow cover trend results using climate scenarios for period 2020-2100

For a more detailed analysis of future trends of snow cover, the estimated values for the months of December, January and February are analyzed separately. In fact, snow change trends in the next 80 years are estimated according to the mentioned scenarios for each of the months of the winter season. For brevity, only the graphs for January are illustrated for pixel #5 in Figure 3, and the rest of the trend results are listed in Tables 3, 4, and 5 for December, January, and February, respectively.

According to the obtained results, at many study points for December, January, and February in the RCP2.6 scenario, considered an optimistic scenario, the predicted trend is an increasing trend and snow cover is expected to increase in the future. In some cases, snow

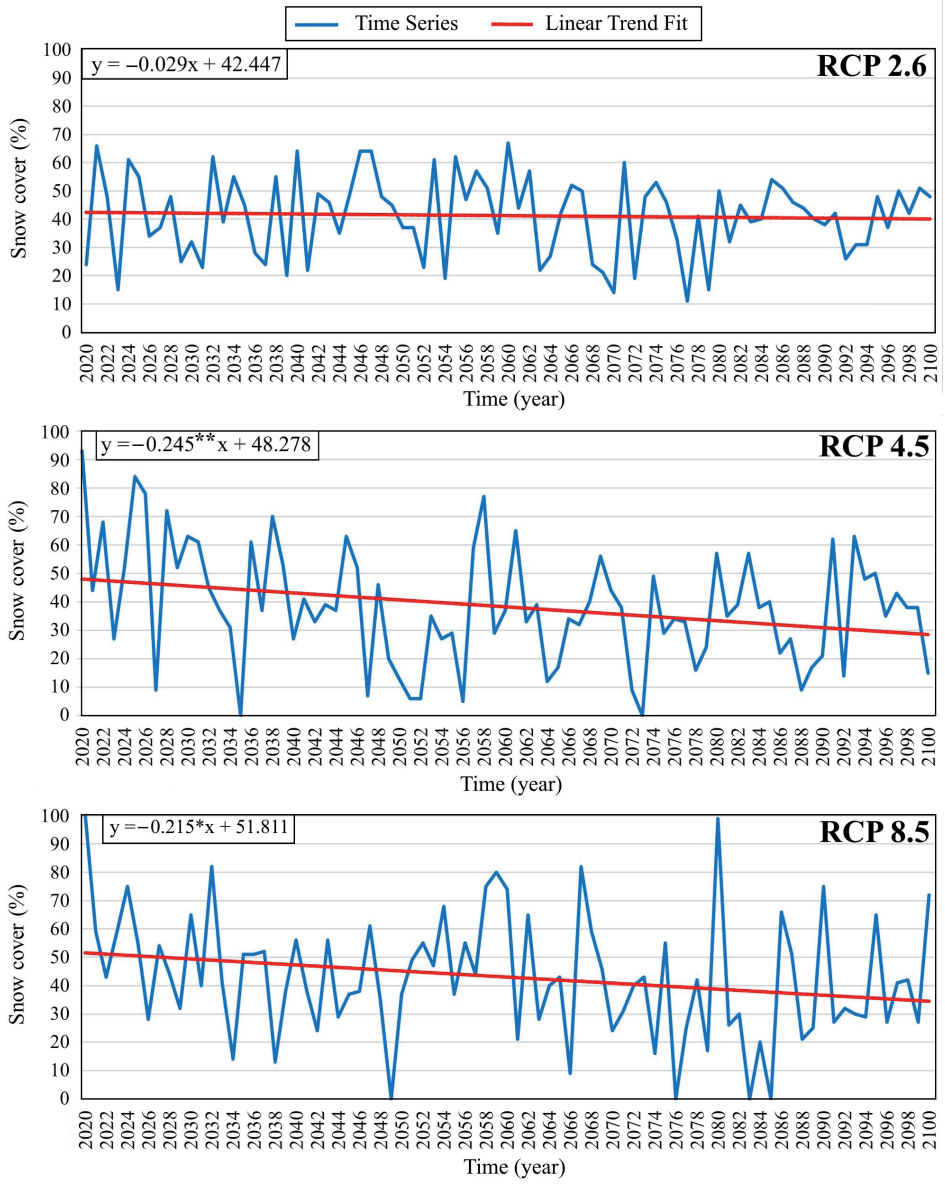

Fig. 3 - Prediction of snow cover for January of 2020-2100 according to the three scenarios at pixel #5 located in Mahneshan-Angoran sub-basin, shown in Figure 1. Note that "" and "**" beside the estimated slopes mean the slopes are statistically significant at 95% and 99% confidence level, respectively*

Pixel	RCP 2.6		RCP 4.5		RCP 8.5	
	slope	p-value	slope	p-value	slope	p-value
1	0.016	0.803	-0.020	0.676	-0.078	0.072
2	0.039	0.625	-0.070	0.329	-0.220	0.002
3	0.025	0.747	-0.034	0.627	-0.230	0.000
4	-0.051	0.403	0.003	0.959	-0.080	0.081
5	-0.045	0.597	0.070	0.344	-0.240	0.011
6	-0.088	0.202	-0.062	0.313	-0.460	0.000
7	0.115	0.778	-0.013	0.749	-0.066	0.134
8	0.120	0.073	-0.150	0.023	-0.180	0.021
9	-0.019	0.574	-0.110	0.002	-0.250	0.000
10	-0.023	0.643	-0.114	0.024	-0.170	0.003
11	-0.085	0.205	0.043	0.559	-0.210	0.003

Tab. 3 - The estimated slopes and their p-values for snow cover time series for December of 2020-2100

Pixel	RCP 2.6		RCP 4.5		RCP 8.5	
	slope	p-value	slope	p-value	slope	p-value
1	0.071	0.244	-0.110	0.110	-0.052	0.350
2	-0.024	0.714	-0.151	0.062	-0.125	0.086
3	-0.104	0.100	-0.340	0.000	-0.270	0.000
4	-0.082	0.180	-0.058	0.445	-0.047	0.424
5	-0.030	0.670	-0.240	0.011	-0.220	0.037
6	-0.010	0.874	-0.026	0.003	-0.380	0.000
7	0.130	0.023	-0.110	0.007	-0.100	0.003
8	0.080	0.290	-0.210	0.013	-0.150	0.040
9	0.021	0.636	-0.160	0.001	-0.260	0.000
10	0.096	0.077	-0.200	0.001	-0.220	0.001
11	-0.093	0.109	-0.090	0.314	-0.170	0.015

Tab. 4 - The estimated slopes and their p-values for snow cover time series for January of 2020-2100

Pixel	RCP 2.6		RCP 4.5		RCP 8.5	
	slope	p-value	slope	p-value	slope	p-value
1	0.016	0.853	-0.150	0.118	-0.160	0.019
2	-0.059	0.471	-0.170	0.054	-0.280	0.001
3	-0.015	0.844	-0.130	0.172	-0.300	0.000
4	0.017	0.832	-0.120	0.212	-0.200	0.004
5	0.180	0.059	-0.140	0.145	-0.440	0.000
6	0.020	0.806	-0.220	0.008	-0.430	0.000
7	-0.070	0.296	-0.110	0.013	-0.046	0.307
8	-0.079	0.350	-0.110	0.113	-0.150	0.054
9	-0.078	0.099	-0.130	0.003	-0.230	0.000
10	-0.049	0.353	-0.136	0.013	-0.160	0.004
11	0.077	0.282	-0.104	0.169	-0.350	0.000

Tab. 5 - The estimated slopes and their p-values for snow cover time series for February of 2020-2100

cover is expected to have a downward trend. These results and charts of the RCP2.6 scenario and its increasing trend are acceptable and expected due to the nature of this scenario.

The results of the forecast of snow cover for the months of December, January and February under the RCP8.5 scenario show that in all cases snow cover experience a decreasing trend and considering that this scenario is a pessimistic scenario, the decreasing trend has a relatively high slope. Considering the similarity of the results obtained from this scenario and the matching of its decreasing trend with the decreasing trend that occurred in the past, it can be concluded that this scenario and its results are more likely closer to the reality.

The RCP4.5 scenario, an intermediate scenario, considers future conditions to be more normal and does not show a steady trend in forecasting compared to the other two scenarios.

DISCUSSION AND CONCLUSIONS

In the present study, by applying statistical downscaling models and using climatic parameters, snow cover was forecast in the Sefid-Rud basin. Based on the analysis of the relationship between the climatic parameters and the snow cover of different pixels, the number of climatic parameters affecting the snow area in different regions varied from 2 to 6 parameters. However, parameters, such as temperature, wind speed at the surface and higher levels of the atmosphere, direction of wind speed at the surface and higher levels and absolute humidity were the most frequent and influential parameters. It appears that the most influential parameter on snow cover changes and its reduction during the statistical period was temperature because its effect was significant at most of the tested pixels. The validation operation performed on the results of this test confirmed the regression and correlation relationships between the snow area in the test samples and the climatic parameters, providing an acceptable result. The most important issue in the current research was to investigate the role of climate change in snow cover changes, the results of which indicated that a number of climatic parameters, particularly temperature, were influential in the process of snow cover changes.

The role of climate change in reducing snow cover has been confirmed in other studies. Karimi (2013), Najafi Dastanai (2015), Fatahi & Moghimi (2017) and Parandeh Khozani (2016) have investigated this issue in different regions of Iran. Keikhosravi Kiani and Masoudian (2018) have also confirmed the role of temperature in snow cover change in the whole of Iran. Haijom *et alii* (2019) have pointed out the effect of climate change on the reduction of snow cover in China. Shafiq *et alii* (2018) in Indian Kashmir and Ahmed *et alii* (2018) in Pakistan have acknowledged the role of climate change in increasing snow cover.

Among the climate scenarios, the RCP2.6 scenario predicted an increase in snow cover. While the two scenarios of RCP4.5 and RCP8.5, particularly the RCP8.5 scenario, predicted snow cover with a decreasing trend due to the increase in temperature. Considering that in most times of the year, snow area of the pixels in question was zero or had no snow cover, the process of investigating the relationship between snow cover and climatic parameters and its prediction proved difficult. Nevertheless, it can be concluded that snow cover will decrease at the Sefid-Rud basin in the future based on current climatic parameter trends and global warming as well as the results obtained from the different stages of this research.

REFERENCES

Aghelpour P., Guan Y., Bahrami-Pichaghchi H., Mohammadi B., Kisi O. & Zhang D. (2020) - *Using the MODIS Sensor for Snow Cover Modeling and the Assessment of Drought Effects on Snow Cover in a Mountainous Area.* Remote Sensing, **12**: 3437.

Ahmad S., Israr M., Liu Sh., Hayat H., Gul J., Wajid S., Ashraf M., Baig S., U. Tahir, A A. (2018) - *Spatio-Temporal Trends in Snow Extent and Their Linkage to Hydro-Climatological and Topographical Factors in the Chitral River Basin (Hindukush, Pakistan)*. Geocarto International, **35**: 711-734.

Ahmed M.R., Ghaderpour E., Gupta A., Dewan A. & Hassan Q.K. (2023) - *Opportunities and Challenges of Spaceborne Sensors in Delineating Land Surface Temperature Trends: A Review*. IEEE Sensors Journal, **23**: 6460-6472.

Arabi Aliabad F., Zare M., Ghafarian Malairia H., Pouriyeh A., Shahabi H., Ghaderpour E. & Mazzanti P. (2024) - *Reconstructing Daytime and Nighttime MODIS Land Surface Temperature in Desert Areas Using Multi-Channel Singular Spectrum Analysis.* Ecological Informatics, **83**: 102830.

Boudala F.S., Milbrandt J.A. & Isaac G.A. (2022) - *Evaluation of CanESM Cloudiness, Cloud Type and Cloud Radiative Forcing Climatologies Using the CALIPSO-GOCCP and CERES Datasets.* Remote Sensing, **14**: 3668.

Dietz A, J., Kuenzer C., Gessner U. & Dech S. (2012) - *Remote Sensing of Snow–A Review of Available Methods.* International Journal of Remote Sensing, **33**: 4094-4134.

Entezami H., Mojarrad F., Shahabi H. & Ghaderpour E. (2024) - *Spatiotemporal Variability in Snow and Land Cover in Sefid-Rud Basin, Iran*. Sustainability, **16**: 9381.

Fattahi E. & Moghimi Sh. (2019) - *Investigation of Snow Cover Changes Affected by Climate Change in North West of Iran*, Scientific Journals Management System, **19**(54): 47-63.

Ghaderpour E., Mazzanti P., Bozzano F. & Scarascia Mugnozza G. (2024) - *Trend Analysis of MODIS Land Surface Temperature and Land Cover in Central Italy.* Land. Vol., **13**: 796.

Ghaderpour E., Mazzanti P., Scarascia Mugnozza G. & Bozzano F. (2023) - *Coherency and phase delay analyses between land cover and climate across Italy via the least-squares wavelet software*. Int. J. Appl. Earth Obs. Geoinf., **118**: 103241.

Gulizia C. & Camilloni I. (2015) - *Comparative Analysis of The Ability of A Set of CMIP3 and CMIP5 Global Climate Models to Represent Precipitation in South America*. International Journal of Climatology, **35**: 583-595. DOI: 10.1002/joc.4005.

Haijum D., Yaning CH. & Yang L. (2019) - *Glacier and Snow Variations and Their Impacts on Regional Water Resources in Mountains.* Journal of Geographical Sciences, **29**(1): 84-100.

IPCC (2013) - Climate change 2013: *The physical science basis, contribution of Working Group I to the Fifth Assessment Report of the Intergovernmental Panel on Climate Change (IPCC).* Cambridge: Cambridge University Press.

Karimi N. (2014) - *Analysis of Climate Change Impact on Glacier by Using Remote Sensing Data (Case Study: Alamkouh Glacier)*, Ph.D. Thesis, Department of Physical Geography, Faculty of Humanities, Tarbiat Modarres University. Sensing Data. Geography and Development, **15**(49): 189-204.

Khan M., Couldlibali P. & Dibike Y. (2006) - *Uncertainty Analysis of Statistical Downscaling Methods*. Journal of Hydrology, **319**: 357-382.

Kulkarni A. V., Rathore B. P., Singh S. K. & Bahuguna I. M. (2011) - *Understanding Changes in the Himalayan Cryosphere using Remote Sensing Techniques.* Int. J. Remote Sensing, **32**(3): 601-615.

Laghari A., Vanham D. & Rauch W. (2012) - *To What Extent does Climate Change Result in a Shift in Alpine Hydrology? A Case Study in the Austrian Alps*. Hydrology Science Journal, **57**(1): 103-117.

Malmros J, K., Mernild S H., Wilson R., Tagesson T., Brahmbhatt R. & Fensholt R. (2018) - *Snow Cover and Snow Albedo Changes in the Central Andes of Chile and Argentina from Daily MODIS Observations (2000 -2016).* Remote Sensing of Environment, **209**: 240-252.

Moore T. T. (2011) - *Climate Change and Animal Migration.* Environmental Law, **41**: 393-405.

Muntan E., Garcia C., Oller P., Marti G., Garcia A. & Gutierrez E. 2009. *Reconstructing Snow Avalanches in the Southeastern Pyrenees.* Nat. Hazards Earth System Science, **9**: 1599-1612.

Najafi Dastenai Z. (2015) - *Snow Cover Monitoring In a changing Climate Using Remote Sensing (Case Study: Zayandeh Rud Basin)*, M.Sc. thesis, Department of Water Engineering, Faculty of Agricultural Sciences Engineering, Sari Agricultural Sciences and Natural Resources University.

Pachauri, R. K., Allen, M. R., Barros, V. R., Broome, J., Cramer, W., Christ, R., Church, J. A., Clarke, L., Dahe, Q., Dasgupta, P. 2014. *Contribution of Working Groups I, II and III to the Fifth Assessment Report of the Intergovernmental Panel on Climate Change.* Geneva, Switzerland: IPCC. Climate change 2014 Synthesis Report.

Pant, N., Kumar, M., Rawat, J., Rani, N. 2014. *Study of Snow Cover Dynamics of Pinder Watershed in Central Himalaya using Remote Sensing and GIS Techniques*. International Journal of Advanced Remote Sensing and GIS. Vol. 3(1), pp. 122–128.

Parandeh Khozani A. (20169 - *Investigating the Trend of Spatial and Temporal Changes in Snow Cover in Zagros Mountain Region and its Relationship with Atmospheric Circulation Patterns and Climate Changes*. Ph.D. Thesis, Department of Water and Meteorology. Faculty of Planning and Environmental Sciences. Tabriz University.

Rani S. (2017 - *Evaluating Snow Cover Changing Trends of the Western Indian Himalaya*. Spatial Information Research, **26**(1): 103-112.

Riggs G., Hall D., Román M. (2019) - *MODIS Snow Products Collection 6.1 User Guide*; National Snow and Ice Data Center: Boulder, CO, USA.

Salomonson V. V. & Appel I. (2004) - *Estimating Fractional Snow Cover from MODIS Using the Normalized Difference Snow Index*. Remote Sens. Environ., **89**(3): 351-360.

Shafiq M. U., Ahmed P., Islam Z. U., Joshi P. K. & Bhat W. A. 2018. *Snow Cover Area Change and Its Relations with Climatic Variability in Kashmir Himalayas, India.* Geocarto International. Vol. **34**: 688-702. https://doi.org/10.1080/10106049.2018.1469675.

Sharma V., Mishra V. D. & Joshi P. K. (2012) - *Snow Cover Variation and Streamflow Simulation in a Snow-Fed River Basin of the North-West Himalaya.* Jornal of Mountain Science, **9**(6): 853-868.

Shuai Y., Masek J. G., Gao F. & Schaaf C. B. (2011) - *An Algorithm for the Retrieval of 30-M Snow-Free Albedo from Landsat Surface Reflectance and MODIS BRDF.* Remote Sensing of Environment, **115**(9): 2204-2216.

Singh D. K., Gusain H. S., Mishra V. & Gupta N. (2018) - *Snow Cover Variability in North-West Himalaya during Last Decade.* Arabian Journal of Geosciences, **11**(579). https://doi.org/10.1007/s12517-018-3926-3.

Tahir A. A., Chevallier P., Arnaud Y., Ashraf M. & Bhatti M. T. (2015) - *Snow Cover Trend and Hydrological Characteristics of the Astore River Basin (Western Himalayas) and Its Comparison to the Hunza Basin (Karakoram Region).* Science Total Environment, **505**: 748-761.

Taylor K. E., Stouffer R. J. & Meehl G. A. (2012) - *An Overview of CMIP5 and the Experiment Design.* Bulletin of the American Meteorological Society: 485-498. DOI: 10.1175/BAMS-D-11-00094.1

Vanham D. (2012) - *The Alps under Climate Change: Implications for Water Management in Europe.* Jornal Water Climate Change, **3**(3): 197-206.

Zaghloul M.S., Ghaderpour E., Dastour H., Farjad B., Gupta A., Eum H., Achari G. & Hassan Q.K. (2022) - *Long Term Trend Analysis of River Flow and Climate in Northern Canada*. Hydrology, **9**: 197.

Zhao Q., Liu Z., Ye B., Qin Y., Wei Z. & Fang S. (2009) - *A Snowmelt Runoff Forecasting Model Coupling WRF and DHSVM*. Hydrol Earth System Science, **13**:1897-1906.

Received November 2024 - Accepted December2024